Bioorganic Chemistry 91 (2019) 103161

Contents lists available at ScienceDirect

Bioorganic Chemistry

journal homepage: www.elsevier.com/locate/bioorg

Synthesis and biological evaluation of bergenin-1,2,3-triazole hybrids as novel class of anti-mitotic agents

P. Pavan Kumar[a,1], Bandi Siva[a,1], Banoth Venkateswara Rao[a], G. Dileep Kumar[a], V. Lakshma Nayak[b], S. Nishant Jain[b], Ashok K Tiwari[a], U. Purushotham[c], C. Venkata Rao[d], K. Suresh Babu[a,*]

[a] Centre for Natural Products & Traditional Knowledge, CSIR-Indian Institute of Chemical Technology, Hyderabad 500 007, India
[b] Division of Applied Biology, CSIR-Indian Institute of Chemical Technology, Uppal Road, Hyderabad 500607, India
[c] Qstatix Private Limited, Hyderabad 500035, India
[d] Department of Chemistry, Sri Venkateswara University, Tirupati 517502, India

ARTICLE INFO

Keywords:
Mallotus philippensis
Bergenin
1,2,3-Triazole hybrids
Cytotoxic activity

ABSTRACT

In continuation of our investigation of pharmacologically-motivated natural products, we have isolated bergenin (**1**) as a major compound from *Mallotus philippensis*, which is deployed in different Indian traditional systems of medicine. Here, a series of bergenin-1,2,3-triazole hybrids were synthesized and evaluated for their potentials against a panel of cancer cell lines. Several of the hybrid derivatives were found more potent in comparison to parent compound bergenin (**1**). Among them, **4j** demonstrated potent activity against A-549 and HeLa cell lines with IC_{50} values of **1.86** μM and **1.33** μM, respectively, and was equipotent to doxorubicin. Cell cycle analysis showed that **4j** arrested HeLa cells at G2/M phase and lead to accumulation of Cyclin B1 protein. Cell based tubulin polymerization assays and docking studies demonstrated that **4j** disrupts tubulin assembly by occupying colchicine binding pocket of tubulin.

1. Introduction

Despite efforts to eliminate cancer in the past decade, disease remains a life threatening one and ranks second to the heart disease worldwide [1]. As per the latest statistical data by International Agency for Research on Cancer (IARC), global cancer burden is estimated to have risen to 18.1 million with 9.6 million deaths in 2018 [2]. As an integral part of all modern drug discovery process from the past few decades, many therapeutic strategies were developed for clinical management of cancer patients which include radiation therapy, chemotherapy and surgery [3]. Todate, chemotherapy remains frontline therapy of choice for combating cancer even after several decades of drug development efforts. On the other hand, clinical effectiveness of currently available anti-cancer agents has been hampered by side effects including drug resistance and toxicity [4]. These drawbacks necessitates development of new therapeutic agents. In this context, natural products are well recognized as a rich source of bioactive compounds and annunciate ~74% of marketed drugs, in terms of chemotherapy or prevention [5]. Moreover, commercially available agents such as vinblastine, vincristine, vinorelbine, etoposide, teniposide, paclitaxel, docetaxel, topotecan and irinotecan are either based on plant or marine sources.

In the course of our continuous efforts during the last two decades in discovery and identification of bioactive leads from traditional Indian flora [6–8], we have set-up and validated original screening in conjunction with classical medicinal chemistry approach for finding more effective analogs with novel mechanisms of action [9]. We adopted this strategy in the present investigation for identification of bergenin as a natural lead compound (Fig. 1). Structurally, bergenin represents a dihydroisocoumarin derivative, which has demonstrated wide range of biological activities including anti-inflammatory, antioxidant, hepatoprotective, neuroprotective, anti-HIV, antiarrhythmic, antifungal, and gastroprotective activities antimalarial, insecticidal, and most recently anticancer activity [10]. Besides its versatile biological activities, bergenin also harbours few side effects, low toxicity and lack of drug resistance. Consequently, several approaches have been devised either to derivatize molecules or synthesize its related compounds to optimize them as lead molecule [11,12]. Recently, concept of hybrid molecules

* Corresponding author.
E-mail address: suresh@iict.res.in (K. Suresh Babu).
[1] Equal contribution.

https://doi.org/10.1016/j.bioorg.2019.103161
Received 26 April 2019; Received in revised form 26 July 2019; Accepted 27 July 2019
Available online 31 July 2019

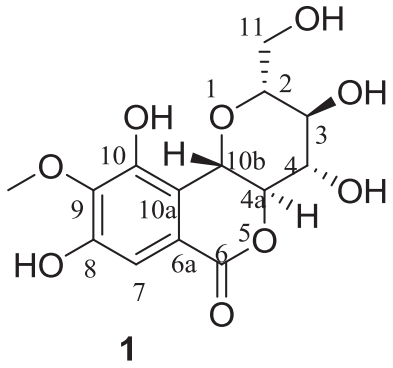

Fig. 1. Isolated Bergenin(**1**) structure.

in which two or more pharmacophores are covalently linked together, have emerged as moving approach in discovery of new cytotoxic agents as they are purported to dilute undesirable effects compared to parent compounds [13,14].

Thus, in continuation of our recent work on bergenin analogs, present study was devised to synthesize a series of bergnin-1,2,3-triazole hybrids using click reaction protocol [15] and investigate their anticancer activities against panel of cancer cell lines. We have also extended our efforts to establish structure-activity relationships within this biologically interesting class of compounds, both to ascertain potential directions for synthetic lead-optimization studies, as well as to identify an optimal candidate among currently available compounds for *in vitro* studies. Herein, we report synthesis of bergenin-triazole hybrids and their results of *in vitro* cytotoxic potentials.

2. Results and discussion

2.1. Chemistry

As part of pharmacological-phytochemical integrated studies, from *Malltous phillippensis*, we isolated and identified bergenin as lead compound in good yield with profound cytotoxic activity against battery of cancer cell lines. Large quantities coupled with its functionalities prompted us to focus on semisynthetic derivatization for development of more efficacious compounds. In view of the fact that free hydroxyl groups are essential for activity through hydrogen bonding in the lead molecules, we focused on synthesis of new analogues by keeping intact hydroxyl groups. It is well known that 1,2,3-triazole pharmacophore found in a number of biologically active compounds posses diverse biological activities such as anti-HIV, antibiotics, antiviral, and anticancer. Based on this core reason, we focussed on exploration of H-7 for preparation of bergenin-triazole hybrids through a Huisgen 1,3-dipolar cycloaddition reaction (click reaction) of alkynes and azides. The route for synthesis of target compounds (**4a-4m**) is illustrated in Scheme 1. Initially, piperazine was treated with propargyl bromide in THF in the presence of cesium carbonate (Cs_2CO_3) to obtain compound 2. In step 2, bergenin was treated with compound **2** in presence of 37% formaldehyde in DMSO [16] at 50 °C for 12 h under Mannich reaction

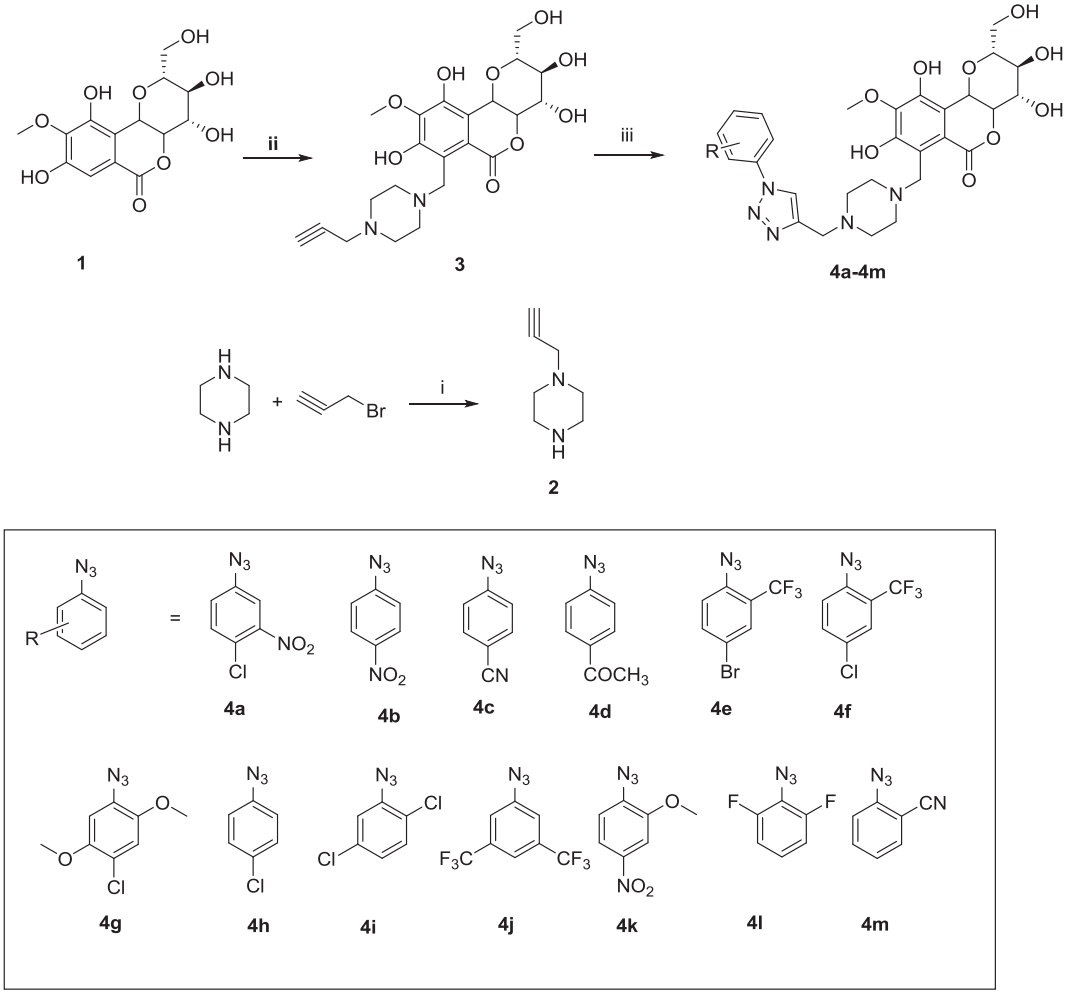

Scheme 1. Reagents and conditions: (i) Propargyl bromide, Cs_2CO_3, THF, rt, 12 h; 68% (ii)37% HCHO, DMSO, 50 °C, 12 h, 60%; (iii) R-N_3, CuI, THF, 90 °C, 12 h, 80–95%.

Table 1
IC_{50} values[a] (in μM) for compounds (**4a-4m**).

Compounds	DU-145[b]	A549[c]	HCT 116[d]	HepG2[e]	HeLa[f]
1	54.43 ± 3.51	34.29 ± 1.59	44.12 ± 0.58	60.91 ± 3.96	22 ± 2.11
4a	28.514 ± 1.39	11.568 ± 0.41	18.290 ± 2.53	12.770 ± 1.35	12.3 ± 1.36
4b	35.423 ± 4.27	16.581 ± 1.29	51.330 ± 2.50	12.750 ± 0.83	9.8 ± 1.7
4c	48.100 ± 0.14	9.921 ± 1.02	21.292 ± 0.74	15.418 ± 1.92	8.12 ± 0.61
4d	41.278 ± 2.79	23.047 ± 0.87	11.945 ± 0.73	30.545 ± 0.50	12.36 ± 1.54
4e	80.832 ± 2.33	22.801 ± 3.18	31.417 ± 45	15.727 ± 4.23	21.25 ± 1.4
4f	20.274 ± 1.60	4.938 ± 0.54	13.375 ± 3.81	10.995 ± 2.24	7.89 ± 1.31
4g	20.974 ± 0.67	6.392 ± 0.34	11.218 ± 3.42	20.881 ± 1.36	6.91 ± 1.36
4h	38.527 ± 3.15	8.142 ± 0.02	27.235 ± 1.26	18.105 ± 3.11	7.36 ± 2.45
4i	64.080 ± 3.22	23.303 ± 1.69	26.104 ± 4.25	38.826 ± 1.07	14.1 ± 2.63
4j	13.939 ± 0.38	1.864 ± 0.12	112.120 ± 1.74	11.128 ± 1.50	1.33 ± 0.68
4k	14.271 ± 0.76	7.111 ± 0.64	19.947 ± 2.77	10.385 ± 0.50	4.7 ± 0.58
4l	28.669 ± 3.23	8.223 ± 0.54	19.470 ± 2.93	21.925 ± 0.68	6.5 ± 0.97
4m	40.473 ± 3.31	11.132 ± 2.89	18.617 ± 0.25	23.850 ± 1.52	9.58 ± 1.2
Doxorubicin	1.260 ± 0.17	1.976 ± 0.16	0.873 ± 0.21	1.704 ± 0.41	1.34 ± 0.32

[a] 50% Inhibitory concentration after 48 h of drug treatment.
[b] Human prostate cancer.
[c] Human lung cancer.
[d] Human colon cancer.
[e] Human liver cancer.
[f] Human cervical cancer.

conditions to yield terminal alkyne derivative (**3**). Finally, bergenin having terminal alkyne product (**3**) was treated with a series of azides in standard Cu(I)-catalyzed alkyne-azide [3 + 2] cyclo addition, known as click reaction, to afford target compounds (**4a-4m**) in good yields. Azides used in click reaction were synthesized in few steps from simple precursors following known reaction procedures. All triazole derivatives were purified through silica gel column chromatography and were fully characterized by IR, NMR and high-resolution mass spectral (HRMS) analysis (see Supporting information). In ^{1}H NMR spectra, the characteristic signal for hydrogen present in triazolic ring was observed within the δ 8.00–8.75 ppm range in all the products and carbon chemical shifts were also compatible with the structures of target compounds.

2.2. Biological activity

Bergenin-triazole hybrids were evaluated for their cytotoxicity against panel of cancer cell lines *viz.* DU-145, A549, HCT-116, HepG2 and Hela cells. The anticancer drug doxorubicin was used as positive control [17]. Results presented in Table 1 represent average of three independent experiments. It is evident from Table 1, that majority of synthetic derivatives displayed better cytotoxic activity than parent compound**1** on A 549, HepG2 and HeLa cell lines. Except compounds **4e** and **4i** on DU-145 cells, and **4b** and **4j** on HCT 116 cell activity of other derivatives presented better cytotoxicity levels on these cell lines than bergenin (Table 1). Among the library of compounds tested, compound **4j** showed potent activity against A549 and HeLa cell lines with the IC_{50} of **1.86** μM and **1.33** μM respectively, which is comparable to the standard drug, doxorubicin (IC_{50} values 1.98 μM and 1.34 μM respectively). Preliminary structure-activity relationship indicates that presence of a substituent such as a chlorine atom or a cyano, floro and CF_3 group on aromatic triazole partner enhanced activity with IC_{50} values ranging from 1.33 to 9.9 μM on A459 cell as well as HeLa cell lines within the studied series. Therefore, compound **4j** was further investigated to explore underlying mechanism of cell death induction. We chose HeLa cell lines to perform these experiments.

2.2.1. *4j arrests cells in G2/M phase*

Most of the anti-cancer agents manifest their activity by obliterating tumor cell cycle and thereby inducing apoptosis [18]. Hence, to understand whether **4j** treatments cause cell cycle arrest, HeLa cells were treated with compound for 18 h. Flow cytometry analysis was performed to analyze cell profile in **4j** treated cells. DMSO treated cells showed that most of the cells accumulated in G1 phase, a characteristic feature of growing tumor cells. The nocodazole or **4j** cells however, accumulated in G2/M as is evidenced by the increase in percentage cell populations (Fig. 2). In addition, higher 8 N nuclei population of cells were also observed in 4j as was found in case of nocodazole treated cells. Finally, **4j** treatment resulted in the arrest of cells in G2/M phase similar to nocodazole, an anti-mitotic agent.

2.2.2. *4j disrupts microtubule network of HeLa cells*

Since bergenin arrested cell growth, we made effort to check cellular morphology [19]. To elucidate this, we treated HeLa cells were treated with **4j** or nocodazole for 18 h and analyzed for cellular microtubule architecture. Changes in the morphology of drug-treated cells present variation in microtubule network. It was interesting to observe that, bergenin and nocodazole treated cells showed rounded morphology (Fig. 3), the characteristic feature of mitotic arrest. DAPI was used to counter stain nucleus. Our results indicate that **4j** treated cells undergo mitotic arrest with a profound change in microtubule architecture.

2.2.3. *Tubulin polymerization assay*

4j treatments showed a drastic change in cell morphology, which is reminiscent of nocodazole or anti-mitotic agents induced change in cell phenotype. Moreover, anti-mitotic agents predominantly modulate cellular tubulin assembly to manifest their effects [20], hence we checked if tubulin was a **4j** target. For this, we assessed homeostasis of polymerized versus soluble tubulin protein in **4j**, nocodazole or paclitaxel treated cells. HeLa cells were treated with **4j** or anti-mitotic agents or DMSO for 18 h and subsequently harvested into soluble and polymerized fractions. Both the fractions were solublized in sample buffer, equal amounts of protein were separated in SDS-PAGE and immunoblotted for tubulin protein. DMSO-treated cells showed fairly equal amounts of protein in both the fractions, whereas marked shift of tubulin protein to soluble fraction was observed in **4j** or nocodazole treated cells (Fig. 4). Whereas, paclitaxel treated cells showed more tubulin protein in insoluble fraction (Fig. 4), because paclitaxel promotes tubulin assembly. Therefore, our results suggest that **4j** inhibits tubulin polymerization and possibly arrests cells in G2/M.

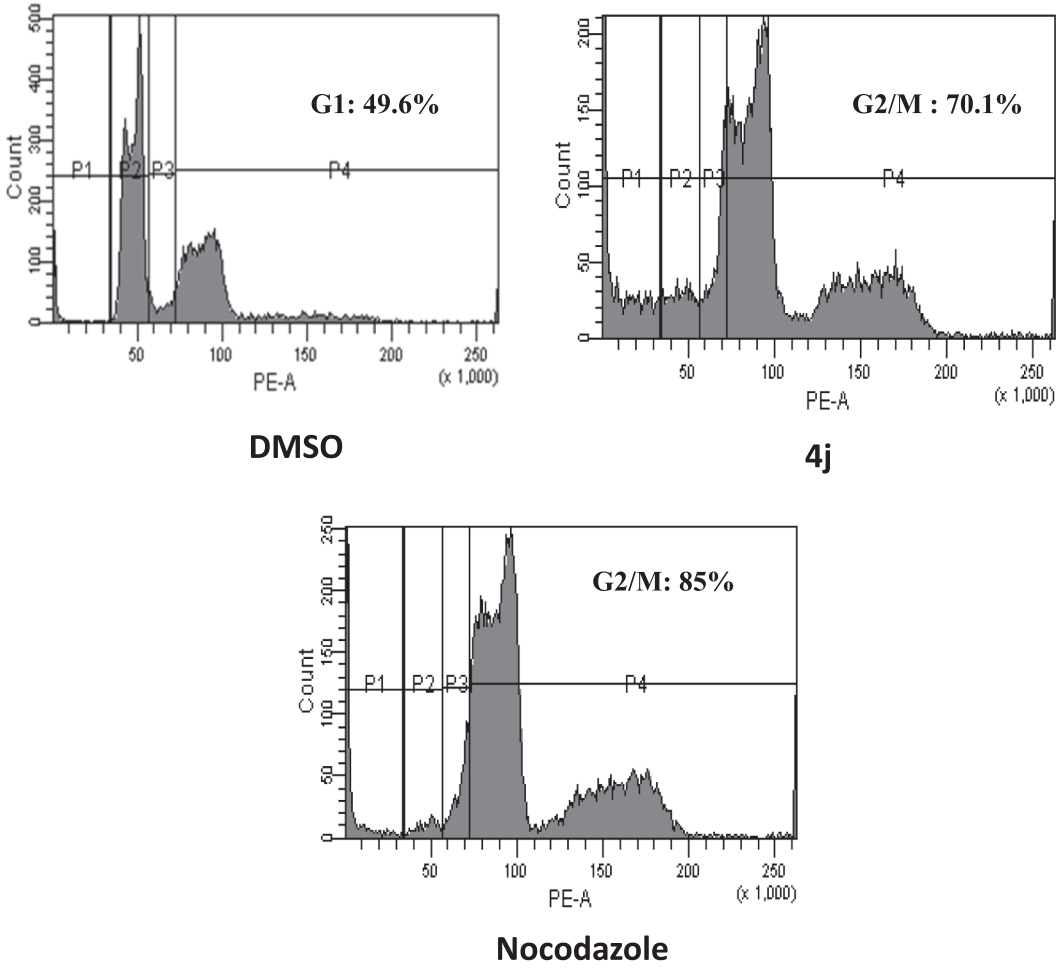

Fig. 2. Hela cells were treated with indicated compounds for 18 h and analyzed for cell cycle profile. DMSO-treated cells show a drastic accumulation in G1, whereas **4j** or nocodazole treated cells show a marked accumulation of cells in G2/M.

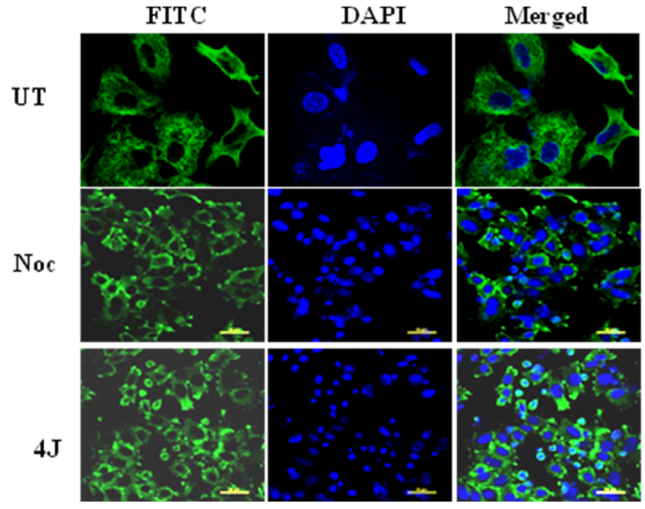

Fig. 3. Hela cells were treated with **4j** or nocodazole or left untreated for 18 h. Later cells were fixed and stained for tubulin and imaged under a confocal microscope. DAPI was used as a counterstain.

2.2.4. *4j treatments induce Cyclin-B1 protein levels*

CyclinB-1 is a master regulator of mitosis, and its protein levels peak during cell division or treatments with anti-mitotic agents [21]. To substantiate our observations, that **4j** treatments result in G2/M arrest, we treated HeLa cells with **4j** or nocodazole or paclitaxel for 18 h.

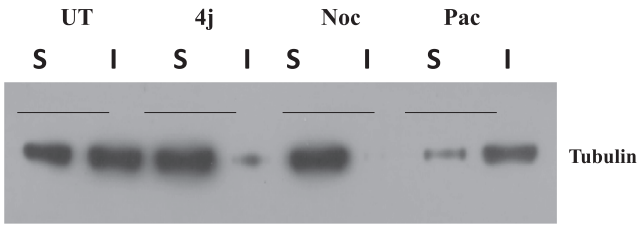

Fig. 4. Effect of compound **4j** on microtubule and nuclear condensation: HeLa cells were treated with 1 μM of **4j** or 0.1 μM of Noc, or Paclitaxel for 24 h. Later, collected the soluble and insoluble fraction of tubulin, and then subjected to western blotting. Soluble fraction of tubulin was more in berginin treated cells. Nocadazole and Paclitaxel were used as an reference standards.

Subsequently, the cells were lysed and analyzed for Cyclin-B1 protein levels. Notably, treatments with bergenin induced Cyclin-B1 protein levels similar to nocodazole or paclitaxel treatments (Fig. 5). Finally, our results demonstrate that bergenin mediated cell death is through a profound G2/M arrest due to inhibition of tubulin polymerization. Taken together, the cell cycle analysis, altered cell phenotype and cell based tubulin assembly studies demonstrate that **4j** an anti-mitotic agent.

3. Molecular docking studies

The co-crystal of human tubulin with colchicine (PDB ID: 1SA0) was selected for molecular docking analysis [22]. Docking studies of

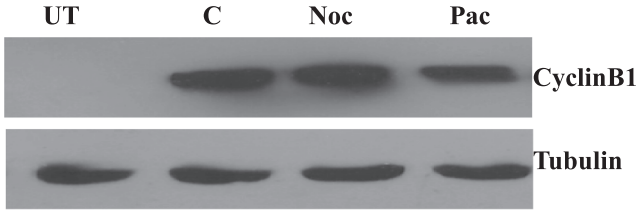

Fig. 5. Western blot analysis for cyclin B1: Protein lysates were collected from HeLa cells, treated with 1 μM of compound **4j** for 24 hr, later subjected to immunoblot analysis. C, represents **4j** significantly induced the Cyclin B1 protein levels.

bergenin, **4j**, nocodazole and doxorubicin molecules were carried out using Autodock software. All four ligands have a core tricyclic ring stabilized by hydrogen bonding interactions in the colchicine-binding site and form hydrophobic interactions with other residues. Further, the oxygen molecules in all ligands make strong hydrogen bonding interactions with Tyr-228, Val-177, Glu-11, Glu-144 and Ile-171 residues of tubulin (Fig. 6). These ligands are mostly stabilized by hydrophobic interactions in the active site. Further, the substituted triazole ring in the **4j** molecule formed hydrogen bonds with Val-177, Tyr-224 and Gly-142 residues. Along with hydrogen bonds the triazole moiety also shows hydrophobic and π-π interactions with Leu-227, Ile-171, Val-204, Asn-206, Ile-231 and Tyr-224 residues (Fig. 6, compound **4j**). We observed that the CF_3 groups on the phenyl ring exhibit strong electrostatic interactions with active site residues. Along with hydrogen bonding, the strong hydrophobic and electrostatic interactions of **4j** ligand results in the molecule more active than other ligands with −10.77 kcal/mol binding energy. The reference doxorubicin and **4j** molecules have similar binding energy values, Table 2 shows **4j** binding strength similar to reference molecule. This suggests that **4j** molecule binds human tubulin at the colchicine-binding pocket with effective hydrogen bonding, electrostatic and hydrophobic interactions which

Table 2
Protein ligand interaction energies (in kcal/mol) calculated by using protein-ligand binding analysis.

Ligand Name	Binding energy (kcal/mol)
Ligand 1	−7.35
Ligand 4j	−10.77
Nocodazole	−7.36
Doxorubucine	−10.08

leads to stable binding. The involvement of **4j** molecule triazole ring interactions with protein leads to have a higher binding energy in comparison to other molecule **1** or nocodazole. Overall, our molecular docking and experimental results corroborate and suggest that **4j** occupies the colchicine-binding site of tubulin, with strong interactions in the binding site.

4. Conclusion

In summary, a series of novel bergenin-trizole hybrid derivatives were synthesized and evaluated their anti-cancer activities against DU-145, A549, HCT-116, Hep G2 and HeLa cell lines. Among tested compounds, **4j** displayed potency in A549 and HeLa cells. Furthermore, the mechanism studies elucidated that compound **4j** triggered cell cycle arrest at the G2/M phase and induced cell apoptosis in a dose- and time-dependent manner. Taken together, compound **4j** effectively inhibited tubulin polymerization, disrupted intracellular tubulin-microtubule balance, resulting prolonged G2/M cell cycle arrest. Docking studies also indicated a strong hydrophobic interaction with tubulin, thus leading to stable binding, consequently leading to apoptosis of cancer cells. As a promising new tubulin-targeting agent, **4j** is worth pursuing for *in vivo* antitumor evaluation as a promising chemotherapeutic agent.

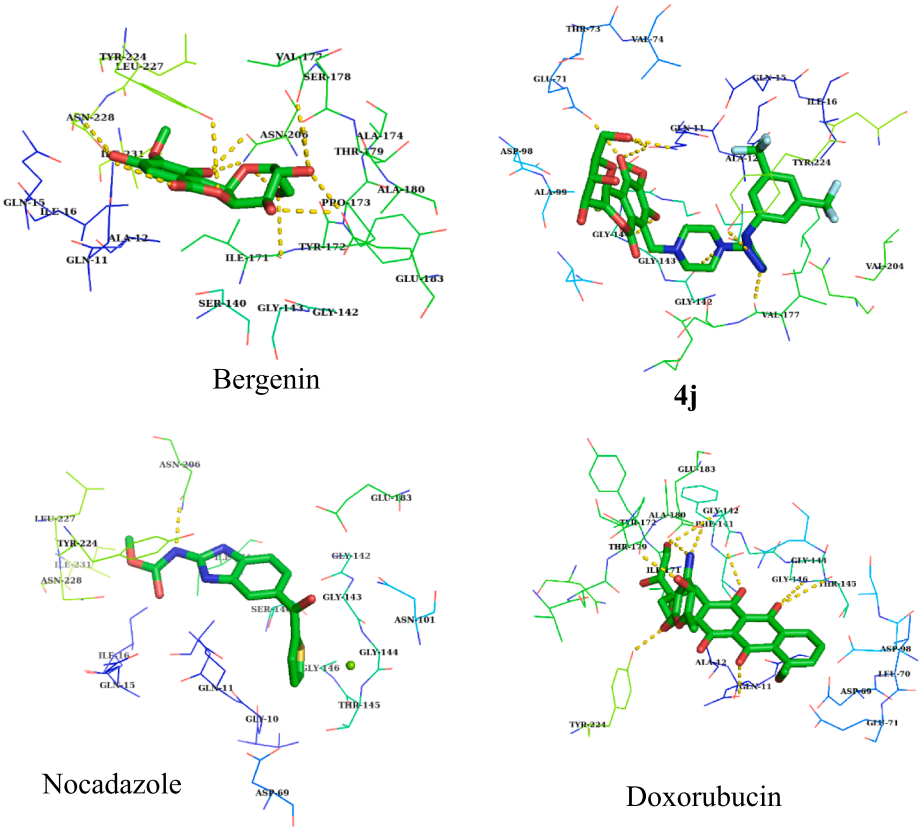

Fig. 6. The representation of the binding site interactions along with residue names of representative four compounds in the human anticancer targets tubulin. Residues within the 5 Å distance from ligand are represented in lines and ligands represented in ball model.

5. Materials and methods

5.1. General

Optical rotations were measured using a JASCO DIP 300 digital polarimeter and at 1 mL cell at 25 °C. IR spectra were recorded on a Nicolet-740 spectrometer with KBr pellets. The NMR spectra were recorded on a Bruker FT-500 MHz spectrometer at 500 MHz for ^{1}H NMR and 75 MHz for ^{13}C NMR respectively, using TMS as internal standard. The chemical shifts are expressed as δ values in parts per million (ppm) and the coupling constants (J) are given in hertz (Hz). Mass spectra were performed on a LC-MS/MS (Agilent Technologies 6510) Q-TOF Mass spectrometer. Column chromatography was performed with silica gel (100–200 mesh), Qing-dao Marine Chemical, Inc., Qingdao, China). Analytical TLC was performed on precoated Merck plates (60 F_{254}, 0.2 mm) and compounds were viewed under a UV lamp (254 and 365 nm) and sprayed with 10% H_2SO_4, followed by heating.

5.2. Plant material

The bark of *Mallotus philliphensis* were collected from Eastern Ghats, AP, India and were authenticated by Dr. K. Madhava Chetty, and a voucher specimen was deposited in the herbarium of Department of Botany, Sri Venkateswara University, Tirupati, Andhra Pradesh, India.

5.3. Extraction and isolation

The dried stem bark of *Mallotus philiphensis* were powdered in a pulvarizer (5 kg) and extracted with methanol at room temperature for 72 h. The resulting extract (150 g) was subjected to column chromatography (using 60–120 silica mesh) eluted successively with $CHCl_3$/MeOH (9:1), $CHCl_3$/MeOH (4:1), to give four fractions F1-F4. Fraction F2 was further purified using column chromatography eluting with $CHCl_3$/MeOH (12:1) to give bergenin as white amorphous powder (15 g), which was identified on the basis of its NMR and mass spectral data.

*Bergenin(**1**):*

*(2R,3S,4S)-3,4,8,10-tetrahydroxy-2-(hydroxymethyl)-9-methoxy-2,3,4,4a- tetrahydropyrano [3,2-c]isochromen-6(10bH)-one(**1**):*

White amorphous Powder; $[\alpha]_D^{25}$ −24.50 (c 0.109, MeOH); IR (KBr)υ_{max}: 3400, 3335, 3279, 2958, 2922, 1707, 1646 cm^{-1}. ^{1}H NMR (500 MHz DMSO-d_6): δ 9.78 (1H, s), 8.45 (1H, s), 6.99(1H, s), 5.65 (1H, d, *J* = 3.9 Hz), 5.44 (1H, s), 4.98 (1H, d, *J* = 10.5 Hz), 4.93 (1H, s), 4.00(1H, t, *J* = 9.9 Hz), 3.83(1H, dd, *J* = 17.3, 6.7 Hz), 3.77(3H, s), 3.66(1H, dd, *J* = 11.9, 5.3 Hz), 3.60–3.52 (1H, m), 3.20 (1H, dd, *J* = 17.1,8.3 Hz); ^{13}C NMR (75 MHz, DMSO-d_6): δ 163.2, 150.8, 147.9, 140.5, 117.9, 115.8, 109.3, 81.6, 79.7, 73.6, 72.0, 70.6, 61.0, 59.7. HRMS (ESI+) *m/z*: 329.0866 ([M+H]$^+$ $C_{14}H_{17}O_9$; calcd. 329.0873).

5.4. General procedure for synthesis of Mannich products (**3**) [16]

To the solution of bergenin (32 mg, 1 mmol) in DMSO (2 mL) was added 37% formaldehyde solution (0.5 mL) and respective secondary amine (1 mmol). The solution was stirred at 50 °C for 8 h, and the mixture was diluted with water and passed through LH-20 resin bed to remove DMSO, and then it was purified over Sephadex LH-20 in methanol to get Mannich products **3** in 60% yield.

*2R,3S,4S)-3,4,8,10-tetrahydroxy-2-(hydroxymethyl)-9-methoxy-7-((4-(prop-2-yn-1-yl)piperazin-1-yl)methyl)-2,3,4,4a-tetrahydropyrano[3,2-c] isochromen-6(10bH)-one(**3**):*

White amorphous powder; yield: 60%; ^{1}H NMR (500 MHz CD_3OD): δ 4.30–4.19 (2H, m), 4.05–3.99 (2H, m), 3.90 (3H, s), 3.84–3.75 (2H, m), 3.71–3.64 (2H, m), 3.41 (1H, t, *J* = 15.5 & 8.3 Hz), 3.36 (1H, d, *J* = 2.20 Hz), 2.74 (8H, brs). ^{13}C NMR (75 MHz CD_3OD) δ 164.9, 154.3, 148.8, 141.3, 118.7, 118.2, 117.6, 82.9, 80.5, 78.7, 75.6, 75.4, 71.8, 62.7, 60.8, 56.8, 53.0, 52.0, 47.1. HRMS (ESI+) *m/z*: 465.1897 ([M+H]$^+$, $C_{22}H_{29}N_2O_9$; calcd. 465.1873).

5.5. General experimental procedure for preparation of compound **4a-4m** [6]

To a stirred solution of **3** (20 mg, 0.038 mmol, 1 equiv) in dry THF (10 mL) was added catalytic amount of flame dried CuI (10 mol %) and appropriate R-N_3 (1.2 equiv) under inert atmosphere and the reaction mixture was refluxed for 12 h. After completion of the reaction (reaction progress was monitored by TLC), the reaction mixture was allowed to cool room temperature, filtered through celite bed and washed with ethyl acetate. The filtrate was concentrated under reduced pressure to get the crude residue, which was further purified by column chromatography using silica gel eluting with chloroform/methanol (90/10) to get the desired products (**4a**-**4m**) in pure form. All synthesized triazole derivatives were confirmed by the spectral analysis FTIR, ^{1}H NMR, ^{13}C NMR and Mass spectroscopy.

5.5.1. (2R,3S,4S)-7-((4-((1-(4-chloro-3-nitrophenyl)-1H-1,2,3-triazol-5-yl) methyl)piperazin-1-yl)methyl)-3,4,8,10-tetrahydroxy-2-(hydroxymethyl)-9-methoxy-2,3,4,4a-tetrahydropyrano [3,2-c]isochromen-6(10bH)-one (**4a**)

Light yellow amorphous powder; yield: 87%; $[\alpha]_D^{25}$ + 2.66 (c 0.090, MeOH); IR (KBr)υ_{max}: 3368, 3302, 2923, 2852, 1645, 1017 cm^{-1}. ^{1}H NMR (300 MHz, CD_3OD): δ 8.61(1H, s), 8.54 (1H, d, *J* = 2.6 Hz), 8.21–8.16 (1H, m), 7.89–7.86 (1H, m), 4.22 (2H, s), 4.04–3.97 (2H, m), 3.89 (3H, s), 3.83–3.76 (2H, m), 3.69–3.64 (2H, m), 3.57 (1H, t, *J* = 8.6 Hz), 2.44 (8H, s); ^{13}C NMR (75 MHz, CD_3OD): δ 164.9, 154.4, 149.9, 148.7, 134.4, 127.0, 125.5, 123.7, 118.5, 118.2, 117.4, 82.9,80.5, 79.2, 78.9, 75.5, 74.4, 71.7, 62.6, 61.0, 60.9,57.5, 57.4, 57.2, 56.2, 53.2, 52.4. HRMS (ESI+) *m/z*: 663.1828 ([M+H]$^+$, $C_{28}H_{32}N_6O_{11}Cl$; calcd.663.1818).

5.5.2. (2R,3S,4S)-3,4,8,10-tetrahydroxy-2-(hydroxymethyl)-9-methoxy-7-((4-((1-(4-nitrophenyl)-1H-1,2,3-triazol-5-yl)methyl)piperazin-1-yl) methyl)-2,3,4,4a-tetrahydropyrano[3,2-c] isochromen-6(10bH)-one (**4b**)

White amorphous powder; yield: 95%; $[\alpha]_D^{25}$ −0.97 (c 0.090, MeOH); IR (KBr)υ_{max}: 3368, 3331, 2947, 2836, 1652, 1453, 1410 cm^{-1}. ^{1}H NMR (500 MHz, CD_3OD): δ 8.55 (1H, s), 8.38–8.32 (2H, m), 8.08–8.04 (2H, m), 4.12 (2H, s), 3.95–3.86 (2H, m), 3.78 (3H, s), 3.73–3.65 (2H, m), 3.60–3.53 (2H, m), 3.30 (1H, t, *J* = 8.4 Hz), 2.63 (4H, s), 2.56 (4H, s); ^{13}C NMR (75 MHz CD_3OD): δ 164.9, 154.4, 148.7,146.0, 142.5, 141.4, 126.5, 123.8, 121.8, 118.2, 117.5, 82.9, 80.5, 75.6, 74.4, 71.8, 62.6, 60.8, 56.9, 53.1, 53.0 ppm. HRMS (ESI+) *m/z*: 629.2203 ([M+H]$^+$, $C_{28}H_{33}N_6O_{11}$; calcd. 629.2207).

5.5.3. 4-(5-((4-(((2R,3S,4S)-3,4,8,10-tetrahydroxy-2-(hydroxymethyl)-9-methoxy-6-oxo-2,3,4,4a,6,10b-hexahydropyrano[3,2-c]isochromen-7-yl)methyl)piperazin-1-yl)methyl)-1H-1,2,3-triazol-1-yl)benzonitrile (**4c**)

White amorphous powder; yield: 83%; $[\alpha]_D^{25}$ −32.29 (c 0.245, MeOH); IR(KBr)υ_{max}: 3406, 3365, 2922, 2854, 2400, 1715 cm^{-1}. ^{1}H NMR (500 MHz, CD_3OD): δ 8.58 (1H, s), 8.09–8.06 (2H, m),7.95–7.92 (2H, m), 4.18 (2H, s), 4.01–3.95 (2H, m), 3.85 (3H, s), 3.80–3.75 (2H, m), 3.67–3.62 (2H, m), 3.38 (1H, t, *J* = 8.8, 18 Hz), 2.67 (8H, brs); ^{13}C NMR(75 MHz CD_3OD) δ 165.1,154.7, 148.8, 146.0, 141.55, 141.50, 135.4, 123.8, 122.0, 119.0, 118.7, 118.5, 117.6, 113.6, 83.0, 80.7, 79.6, 75.7, 74.6, 72.0, 62.8, 61.0, 57.2, 53.38, 53.31 ppm. HRMS (ESI+) *m/z*: 609.2306 ([M+H]$^+$ $C_{29}H_{33}N_6O_9$; calcd. 609.2309).

5.5.4. (2R,3S,4S)-7-((4-((1-(4-acetylphenyl)-1H-1,2,3-triazol-5-yl) methyl)piperazin-1-yl)methyl)-3,4,8,10-tetrahydroxy-2-(hydroxymethyl)-9-methoxy-2,3,4,4a-tetrahydropyrano[3,2-c]isochromen-6(10bH)-one (**4d**)

White amorphous powder; yield: 93%; $[\alpha]_D^{25}$ −10.98 (c 0.272, MeOH); IR (KBr)υ_{max}: 3363, 2922, 2852, 1713, 1680 cm^{-1}. ^{1}H NMR (500 MHz, CD_3OD): δ 8.49 (1H, s), 8.14–8.07 (2H, m), 7.96–7.90 (2H, m), 4.20–4.10 (2H, m), 3.95–3.88 (2H, m),3.79 (3H, s), 3.74–3.66 (2H, m), 3.60–3.53 (2H, m), 3.31 (1H, t, *J* = 9.0 Hz), 2.69 (4H, s), 2.59 (4H, s), 2.55 (3H, s); ^{13}C NMR (75 MHz CD_3OD): δ 165.0, 145.7, 138.3,

131.3, 123.6, 121.2, 118.7, 117.6, 82.9, 80.6, 79.5, 75.6, 74.4, 71.8, 62.6, 60.8, 56.8, 53.2, 52.9 ppm. HRMS (ESI+) *m/z*: 626.2458 [M+H]$^+$, $C_{30}H_{36}N_5O_{10}$; calcd. 626.2462).

5.5.5. 2 (2R,3S,4S)-7-((4-((1-(4-bromo-2-(trifluoromethyl)phenyl)-1H-1,2,3-triazol-4-yl)methyl)piperazin-1-yl)methyl)-3,4,8,10-tetrahydroxy-2-(hydroxymethyl)-9-methoxy-2,3,4,4a-tetrahydropyrano[3,2-c]isochromen-6(10bH)-one ***(4e)***

Yellow amorphous powder; yield: 81%; $[\alpha]_D^{25}$ −8.69 (c 0.181, MeOH); IR (KBr)υ_{max}: 3402, 3361, 2923, 2855, 1712, 1587 cm^{-1}.^{1}H NMR (300 MHz CD_3OD): δ 8.00 (2H, d, J = 8.5 Hz), 7.96 (1H, d, J = 3.8 Hz), 7.71 (1H, dd, J = 8.5, 2.5 Hz), 4.17 (2H, q, J = 14.6 Hz), 3.95–3.89 (2H, m), 3.81 (3H, s), 3.68 (2H, dd, J = 17.0,7.9 Hz), 3.61–3.54 (2H, m), 3.30 (1H, t, J = 8.2 Hz), 2.71 (4H, s), 2.63 (4H, s); ^{13}C NMR (75 MHz, CD_3OD): δ165.0, 154.3, 149.4, 148.9, 141.4, 137.9, 137.7, 132.3, 132.2, 132.1, 127.08, 127.04, 124.8, 122.7, 118.7, 117.6, 85.8, 82.9, 80.6, 79.5, 75.6, 74.4, 71.8, 62.7, 60.8, 56.7, 53.5, 53.2, 52.9 ppm. HRMS (ESI+) *m/z*: 730.1328 ([M+H]+, $C_{29}H_{32}N_5O_9BrF_3$; calcd. 730.1336).

5.5.6. (2R,3S,4S)-7-((4-((1-(4-chloro-2-(trifluoromethyl)phenyl)-1H-1,2,3-triazol-5-yl)methyl)piperazin-1-yl)methyl)-3,4,8,10-tetrahydroxy-2-(hydroxymethyl)-9-methoxy-2,3,4,4a-tetrahydropyrano[3,2-c]isochromen-6(10bH)-one ***(4f)***

White amorphous powder; yield: 88%; $[\alpha]_D^{25}$ −5.53 (c 0.909, MeOH); IR (KBr)υ_{max}: 3335, 2925, 2849, 1713, 1582 cm^{-1}. ^{1}H NMR (300 MHz, CD_3OD): δ 8.14 (1H, s), 7.91 (1H, d, J = 2.2 Hz), 7.80 (1H, dd, J = 8.8, 2.4 Hz), 7.57 (1H, d, J = 8.5 Hz), 4.20–4.09 (2H, m), 3.96–3.87 (2H, m), 3.79 (3H, s), 3.74–3.66 (2H, m), 3.57 (2H, q, J = 6.1 Hz), 3.31 (1H, t, J = 8.7 Hz), 2.74–2.44 (8H, brs); ^{13}C NMR (75 MHz, CD_3OD): δ 164.9,154.3, 148.8, 144.7, 141.4, 138.1, 134.8, 134.6, 132.0, 128.9, 128.8, 128.7, 128.6, 128.2, 124.5, 122.3, 118.6, 117.5, 82.9, 80.5, 75.5, 74.4, 71.8, 62.6, 60.8, 56.8, 53.1, 53.0, 52.89, 52.82 ppm. HRMS (ESI+) *m/z*: 686.1846 ([M+H]$^+$, $C_{29}H_{32}N_5O_9ClF_3$; calcd. 686.1841).

5.5.7. (2R,3S,4S)-7-((4-((1-(4-chloro-2,5-dimethoxyphenyl)-1H-1,2,3-triazol-5-yl)methyl) piperazin-1-yl)methyl)-3,4,8,10-tetrahydroxy-2-(hydroxymethyl)-9-methoxy-2,3,4,4a-tetrahydropyrano[3,2-c] isochromen-6(10bH)-one ***(4g)***

Brick red amorphous powder; yield: 92%; $[\alpha]_D^{25}$ −12.74 (c 0.545, MeOH); IR (KBr)υ_{max}: 3345, 2945, 2832, 1710, 1451 cm^{-1}. ^{1}H NMR (500 MHz, CD_3OD): δ 8.21 (1H, s), 7.36 (1H, d, J = 6.0 Hz), 7.24 (1H, t, J = 5.3 Hz), 4.17 (2H, dt, J = 25.1, 12.4 Hz), 3.96–3.88 (2H, m), 3.82–3.78 (2H, m), 3.76 (3H, s), 3.70 (2H, dt, J = 24.5, 9.1 Hz), 3.61–3.54 (2H, m), 3.31(1H, t, J = 8.5 Hz), 2.78(4H, s), 2.59 (4H, s); ^{13}C NMR (75 MHz, CD_3OD): δ 165.0, 150.8, 149.0, 146.8, 141.4, 125.0, 118.8, 117.8, 116.2, 116.0, 114.1, 110.8, 82.9, 80.5, 75.5, 74.4, 71.8, 71.0, 62.6, 61.0, 60.9, 57.5, 57.4, 57.2, 56.2, 53.2, 52.4 ppm. HRMS (ESI+) *m/z*: 678.2174 ([M+H]$^+$ $C_{30}H_{37}N_5O_{11}Cl$; calcd. 678.2178).

5.5.8. (2R,3S,4S)-7-((4-((1-(4-chlorophenyl)-1H-1,2,3-triazol-5-yl) methyl)piperazin-1-yl)methyl)-3,4,8,10-tetrahydroxy-2-(hydroxymethyl)-9-methoxy-2,3,4,4a-tetrahydropyrano[3,2-c]isochromen-6(10bH)-one ***(4h)***

Light yellow amorphous powder; yield: 88%; $[\alpha]_D^{25}$ + 0.86 (c 0.363, $CHCl_3$); ^{1}H NMR (500 MHz, CD_3OD): δ 8.48 (1H, s), 7.89–7.85 (2H, m), 7.61–7.58 (2H, m), 4.28 (2H, dd, J = 8.9, 2.1 Hz), 4.05–4.00 (2H, m), 3.90 (3H, s), 3.80 (2H, dd, J = 18.4, 9.5 Hz), 3.69–3.65 (2H, m), 3.41 (1H, t, J = 8.8 Hz), 2.85 (4H, s), 2.70 (4H, s); ^{13}C NMR (75 MHz, CD_3OD): δ 165.0, 154.2, 149.0, 145.5, 141.4, 137.0,135.6, 131.0, 123.6, 122.9, 118.8, 117.7, 82.9, 80.6, 79.5, 79.3, 79.0, 75.6, 74.4, 71.8, 62.6, 60.9, 56.4, 53.2, 53.1, 52.5 ppm. HRMS (ESI+) *m/z*: 618.1961([M+H]$^+$, $C_{28}H_{33}N_5O_9Cl$; calcd. 618. 1967).

5.5.9. (2R,3S,4S)-7-((4-((1-(2,5-dichlorophenyl)-1H-1,2,3-triazol-5-yl) methyl)piperazin-1-yl)methyl)-3,4,8,10-tetrahydroxy-2-(hydroxymethyl)-9-methoxy-2,3,4,4a-tetrahydropyrano[3,2-c]isochromen-6(10bH)-one ***(4i)***

Yellow amorphous powder; yield: 87%; $[\alpha]_D^{25}$ −4.72 (c 0.727, MeOH); IR (KBr)υ_{max}: 3343, 2945, 2833, 1692, 1450 cm^{-1}. ^{1}H NMR (500 MHz, CD_3OD): δ 8.23 (1H, s), 7.66–7.63 (1H, m), 7.59 (1H, dd, J = 8.7, 1.5 Hz), 7.54–7.50 (1H, m), 4.19 (2H, dd, J = 17.6, 8.3 Hz), 3.95–3.90 (2H, m), 3.81(3H, s), 3.70 (2H, dt, J = 13.9, 8.9 Hz), 3.57 (2H, dd, J = 10.2, 5.2 Hz), 3.31 (1H, t, J = 8.8 Hz), 2.77 (4H, s), 2.59 (4H, s); ^{13}C NMR (75 MHz CD_3OD): δ 165.0, 154.1,149.0, 137.0, 134.7, 133.0, 132.6, 129.1, 129.0, 118.9, 117.8, 83.0, 82.8, 80.6, 80.4, 75.6, 74.4, 74.1, 71.8, 71.0, 62.7, 62.0, 61.0, 60.9, 56.3, 53.2, 53.0, 52.5, 51.6 ppm. HRMS (ESI+) *m/z*: 652.1573 ([M+H] $^+$ $C_{28}H_{32}N_5O_9Cl_2$; calcd. 652.1577).

5.5.10. (2R,3S,4S)-7-((4-((1-(3,5-bis(trifluoromethyl)phenyl)-1H-1,2,3-triazol-5-yl)methyl)piperazin-1-yl)methyl)-3,4,8,10-tetrahydroxy-2-(hydroxymethyl)-9-methoxy-2,3,4,4a-tetrahydropyrano[3,2-c]isochromen-6(10bH)-one ***(4j)***

Yellow amorphous powder; yield: 83%;^{1}H NMR (300 MHz, CD_3OD): δ 8.65 (1H, s), 8.45 (2H, s), 8.04 (1H, d, J = 15.9 Hz), 4.22–4.12 (2H, m), 3.95–3.88 (2H, m), 3.80 (3H, s), 3.76–3.65 (2H, m), 3.57 (2H, q, J = 6.1 Hz), 3.31 (1H, t, J = 8.8 Hz), 2.69 (4H, s), 2.62 (4H, s); ^{13}C NMR (75 MHz, CD_3OD): 165.0, 154.3, 151.7, 148.8, 146.1, 139.7, 134.6, 134.3, 125.3, 124.0, 123.1, 121.8, 118.7, 117.6, 97.3, 82.9, 82.4, 80.5, 79.4, 75.6, 74.4, 71.8, 62.6, 60.8, 56.6, 53.2, 52.8, 49.8 ppm. HRMS (ESI+) *m/z*: 720.2089 ([M+H]$^+$, $C_{30}H_{32}N_5O_9F_6$; calcd. 720.2104).

5.5.11. (2R,3S,4S)-3,4,8,10-tetrahydroxy-2-(hydroxymethyl)-9-methoxy-7-((4-((1-(2-methoxy-4-nitrophenyl)-1H-1,2,3-triazol-5-yl)methyl) piperazin-1-yl)methyl)-2,3,4,4a-tetrahydropyrano[3,2-c]isochromen-6(10bH)-one ***(4k)***

Light yellow amorphous powder; yield: 87%; $[\alpha]_D^{25}$ −24.17 (c 0.545, MeOH); IR (KBr)υ_{max}: 3335, 2955, 2826, 1707,1459 cm^{-1}.^{1}H NMR (500 MHz, CD_3OD): δ 8.38 (1H, s), 8.00 (1H, s), 7.93 (2H, s), 4.11 (2H, s), 3.97 (3H, s), 3.94–3.85 (2H, m), 3.78 (3H, s), 3.71, (2H, t, J = 7.1 Hz), 3.59–3.54 (2H, m), 3.30 (1H, t, J = 8.8 Hz), 2.60 (8H, d, J = 2.4 Hz); ^{13}C NMR (75 MHz, CD_3OD) 164.9, 154.4, 153.0, 150.0, 148.7, 144.4, 141.3, 132.0, 127.4, 126.7, 118.6, 117.4, 117.3, 109.2, 82.9, 80.5, 79.4, 75.6, 74.4, 71.8, 62.6, 60.8, 57.5, 57.0, 53.1, 53.0 ppm. HRMS (ESI+) *m/z*: 659.2312 ([M+H]+, $C_{29}H_{35}N_6O_{12}$; Calcd. 659.2313).

5.5.12. (2R,3S,4S)-7-((4-((1-(2,6-difluorophenyl)-1H-1,2,3-triazol-5-yl) methyl)piperazin-1-yl)methyl)-3,4,8,10-tetrahydroxy-2-(hydroxymethyl)-9-methoxy-2,3,4,4a-tetrahydropyrano[3,2-c]isochromen-6(10bH)-one ***(4l)***

Yellow amorphous powder; yield: 93%; $[\alpha]_D^{25}$ + 0.86 (c 0.363, MeOH); IR (KBr)υ_{max}: 3365, 3319, 2947, 2833, 1664, 1452 cm^{-1}. ^{1}H NMR (500 MHz CD_3OD): δ 8.18 (1H, s), 7.60–7.54 (1H, m), 7.21(2H, d, J = 8.4 Hz), 4.18 (2H, q, J = 14.6 Hz), 3.95–3.90 (2H, m), 3.81(3H, s), 3.70 (2H, dt, J = 13.6, 10.0 Hz), 3.57 (2H, q, J = 6.2 Hz), 3.31(1H, t, J = 8.6 Hz), 2.73 (4H, s), 2.62(4H, s); ^{13}C NMR (75 MHz, CD_3OD): δ165.0, 159.4, 157.4, 148.9, 133.7, 133.6, 118.8, 117.6, 113.8, 133.7, 113.6, 83.0, 80.6, 79.5, 75.6, 74.5, 71.8, 62.7, 60.9, 60.8, 56.7, 53.2, 52.9 ppm. HRMS (ESI+) *m/z*: 620.2170 ([M+H]$^+$, $C_{28}H_{32}N_5O_9F_2$; calcd. 620.2168).

5.5.13. 2-(5-((4-(((2R,3S,4S)-3,4,8,10-tetrahydroxy-2-(hydroxymethyl)-9-methoxy-6-oxo-2,3,4,4a,6,10b-hexahydropyrano[3,2-c]isochromen-7-yl)methyl)piperazin-1-yl)methyl)-1H-1,2,3-triazol-1-yl)benzonitrile ***(4m)***

White amorphous powder; yield: 86%; $[\alpha]_D^{25}$ −32.29 (c 0.245, MeOH); IR (KBr)υ_{max}: 3366, 2922, 2823, 1705, 1641, 1455 cm^{-1}. ^{1}H NMR (500 MHz, CD_3OD): δ 8.38 (1H, s), 7.97–7.85 (1H, m), 7.84–7.79 (1H, m), 7.78–7.69 (1H, m), 7.66–7.62 (1H, m), 4.19–4.10 (2H, m), 3.98–3.85 (2H, m),3.79(3H, s), 3.76–3.65 (2H, m), 3.60–3.53(2H, m),

3.31(1H, t, J = 8.5 Hz), 2.67 (8H, s); ^{13}C NMR (75 MHz, CD_3OD): δ 164.9, 148.8, 135.7, 131.4, 126.9, 126.3, 118.6, 118.4, 117.5, 116.5, 109.1, 82.9, 80.6, 75.6, 74.5, 71.8, 62.7, 60.8, 53.2, 53.1. HRMS (ESI +) m/z: 609.2306 ($[M+H]^+$, $C_{29}H_{33}N_6O_9$; calcd. 609.2309)

5.6. Biology

5.6.1. Anti cancer activity

The lead compound, bergenin and all synthesized compounds were assayed for their cytotoxicity against cancer cell lines HeLa (cervical), A-549 (lung), HCT116 (colon), DU-145 (Prostate), and HepG2 (liver) by using MTT assay [18]. Cells were plated at a density of 10,000 cells per well in 100 μL DMEM media and supplemented with 10% FBS in each well of 96-well microculture plates and incubated for 24 h at 37 °C in a CO_2 incubator. The cells were then exposed to a series of concentrations of the test compounds (10 to 200 μg/mL) and incubated for 48 h. After 48 h of treatment, 10 μL of MTT solution (5 mg/mL in PBS) was added to each well containing 90 μL of the media. The plates were then incubated for 4 h at 37 °C. After incubation, a volume of 200 μL of DMSO was added to each well for 10 min at room temperature. Absorbance was measured at 570 nm using multidetection reader (Synergy 4, Biotek, USA). The mean % of cell viability relative to that of untreated cells was estimated from data of three individual experiments. The IC_{50} value of each compound was calculated by curve fitting method.

5.6.2. Cell cycle analysis

Flow cytometric analysis (FACS) was performed to evaluate the distribution of the cells through the cell cycle phases. HeLa cells were treated with compound **4j** at 1 μM concentration for 48 h. Untreated and treated cells were harvested, washed with phosphate-buffered saline (PBS), fixed in ice-cold 70% ethanol, and stained with propidium iodide (Sigma–Aldrich). Cell-cycle analysis was performed by flow cytometry (Becton Dickinson FACS Caliber instrument) [22].

5.6.3. Hoechst staining

Hela cells were seeded at a density of 10,000 cells over 18 mm cover slips and incubated for 24 h. After incubation, cells were treated with the compound **4j** at 1 μM concentration for 48 h. After 48 h of drug treatment, Hoechst staining assay was performed as described earlier [23]. Cells from each cover slip were captured from randomly selected fields under fluorescent microscope (Olympus microscope) to qualitatively determine the proportion of viable and apoptotic cells based on their relative fluorescence and nuclear fragmentation

5.6.4. Western blot analysis of soluble versus polymerized tubulin and Cyclin-B1 proteins

Cells were seeded in 12-well plates at 1×10^5 cells per well in complete growth medium. Following treatment of cells with the compound **4j** (1 μM) or nocodazole (0.1 μM) for duration of 24 h, cells were washed with PBS and subsequently soluble and insoluble tubulin fractions were collected. To collect the soluble tubulin fractions, cells were permeablized with 200 μL of pre-warmed lysis buffer [80 mM Pipes-KOH (pH 6.8), 1 mM $MgCl_2$, 1 mM EGTA, 0.2% Triton X-100, 10% glycerol, 0.1% protease inhibitor cocktail (Sigma-Aldrich)] and incubated for 3 min at 30 °C. Lysis buffer was gently removed, and mixed with 100 μL of 3 × Laemmli's sample buffer (180 mM Tris-Cl pH 6.8, 6% SDS, 15% glycerol, 7.5% β-mercaptoethanol and 0.01% bromophenol blue). Samples were immediately heated to 95 °C for 3 min. To collect the insoluble tubulin fraction, 300 μL of 1 × Laemmli's sample buffer was added to the remaining cells in each well, and the samples were heated to 95 °C for 3 min. Equal volumes of samples were run on an SDS-10% polyacrylamide gel and were transferred to a nitrocellulose membrane employing semidry transfer at 50 mA for 1 h. Blots were probed with mouse anti-human α-tubulin diluted 1:2,000 mL (T8203, Sigma) and stained with rabbit anti-mouse secondary antibody coupled with horseradish peroxidase, diluted 1:5000 mL (A9044, Sigma). Bands were visualized using an enhanced Chemiluminescence protocol (Pierce) and radiographic film (Kodak) [24]. For CyclinB1 immunoblots cells were treated with indicated compounds for 18 h and blots were probed with Cyclin-B1 antibody (SAB4503502, Sigma) and anti-rabbit-coupled with horseradish peroxidise (A9164, Sigma).

5.7. Immunofluorescence

HeLa cells were seeded on a glass cover slip, incubated for 18 h in with **4j** (1 μM) or nocodazole (0.1 μM). Cells grown on cover slips were fixed in 4% paraformaldehyde for 10 min and permeabilized for 6 min in 1X PBS containing 0.5% Triton X-100 and 0.05% Tween-20. The permeabilized cells were blocked with 4% BSA (Sigma) in PBS for 1 h. Later, the cells were incubated with primary antibody for tubulin (T8203, Sigma) at 1:200 diluted in blocking solution for 4 h at room temperature. The antibodies were then removed, and the cells were washed thrice with PBS. Cells were then incubated with FITC-labeled anti-mouse secondary antibody **(**F0257, Sigma) for 1 h at room temperature. Cells were washed thrice with PBS and mounted in medium containing DAPI. Images were captured using an Olympus confocal microscope and analyzed with Provision software (instrument: FLOW VIEW-FV 1000 Series; software: FV 10 ASW 1.7 Series)

5.8. Molecular docking study

Molecular modelling studies of bergenin and ligand **4j** along with reference molecules Nocodazole and doxorubicin compounds were carried out using Autodock software. Docking of all compounds was carried out on human tubulin at the colchicines binding pocket (PDB ID: 1SA0, chain A). This protein crystal structure was retrieved from protein data bank (PDB). We have used grid box with spacing of 1 Å, and the box parameters as centre: x = 126.808, y = 93.785, z = 13.163 and grid box size: x = 56, y = 36, z = 62. During docking we have generated 20 conformers for each ligand by using default genetic algorithm. In this study, input preparation carried out using MGL tools-1.5.6 and final docking performed in Autodock.

Acknowledgements

The authors gratefully acknowledge keen interest shown by Dr. S. Chandrasekhar, Director, IICT, Hyderabad. This work was financially supported by NaPAHA project grant CSC-0130 from the Council of Scientific and Industrial Research (CSIR), India under CSIR-Network program. PPK and BS thank to CSIR for financial support. IICT Communication No. IICT/Pubs/2019/150.

Appendix A. Supplementary material

Supplementary data to this article can be found online at https://doi.org/10.1016/j.bioorg.2019.103161.

References

[1] American Cancer Society, http://pressroom.cancer.org/releases?item=290 (accessed March 27, 2019.
[2] American Cancer Society. Cancer Facts & Figures 2018.
[3] F. Fiorica, M. Trovò, A. Ottaiano, G. Nasti, I. Carandina, M. Marzola, P.D. Paoli, M. Berretta, Can the addition of radiotherapy postoperatively increase clinical outcome of patients with gastric cancer? A systematic review of the literature and meta-analysis, Oncotarget 9 (2018) 10734–10744.
[4] M. Nikolaou, A. Pavlopoulou, A.G. Georgakilas, E. Kyrodimos, Thechallenge of drug resistance in cancer treatment: acurrent overview, Clin. Exp. Metastasis 35 (2018) 309–318.
[5] Y. Chen, M.G. de Lomana, N. Friedrich, J. Kirchmair, Characterization of the chemical space of known and readily obtainable natural products, J. Chem. Inf. Model. 58 (2018) 1518–1532.
[6] B. Poornima, B. Siva, A. Venkanna, G. Shankaraiah, Jain D. Nishant, K. Yadav, S. Misra, K. Suresh Babu, Novel Gomisin B analogues as potential cytotoxic agents: design, synthesis, biological evaluation and docking studies, Eur. J. Med. Chem. 139

(2017) 441–453.
[7] D. Amujuri, B. Siva, B. Poornima, K. Sirisha, A.V.S. Sarma, V.L. Nayak, A.K. Tiwari, U. Purushotham, K. Suresh Babu, Synthesis and biological evaluation of Schizandrin derivatives as potential anti-cancer Agents, Eur. J. Med. Chem. 149 (2018) 182–192.
[8] B. Siva, A. Venkanna, B. Poornima, J. Boustie, Schnell Bastien, C. Venkata Rao, P. Nishant Jain, K. Usha Rani, Suresh Babu, New Limonoids from seeds of *Cipadessa baccifera*: isolation, synthesis and their antiproliferative activities, Fitoterapia 117 (2017) 34–40.
[9] G. Li, H.X. Lou, Strategies to diversify natural products for drug discovery, Med. Res. Rev. 38 (2018) 1255–1294.
[10] G.B. Bajracharya, Diversity, pharmacology and synthesis of bergenin and its derivatives: potential materials for therapeutic usages, Fitoterapia 101 (2015) 133–152.
[11] T. Vijaya Kumar, Ashok K. Tiwari, A. Robinson, K. Suresh Babu, R. Sateesh Chandra Kumar, D. Anand Kumar, A. Zehra, J. Madhusudna Rao, Synthesis and antiglycation potentials of bergenin derivatives, Bioorg. Med. Chem. Lett. 21 (2011) 4928–4931.
[12] N.-N. Liu, F.-K. Bao, J.-B. Chen, X.-H. Zeng, S,-J, Chi, J,-P, Liu, Synthesis and cytotoxic activities of novel bergenin derivatives, Med. Chem. Res. 23 (2014) 4803–4813.
[13] S. Fortin, G. Bérubé, Advances in the development of hybrid anticancer drugs, Expert Opin. Drug Discov. 8 (2013) 1029–1047.
[14] B. Poornima, B. Siva, G. Shankaraiah, A. Venkanna, L. Nayak, C. Venkata Rao, K. Suresh Babu, Eur. J. Med. Chem. 92 (2015) 449–458.
[15] S.I. Presolski, V.P. Hong, M.G. Finn, Copper-catalyzed azide-alkyne click chemistry for bioconjugation, Curr. Protoc. Chem. Biol. 3 (2011) 153–162.
[16] S.K. Jain, S. Singh, A. Khajuria, S.K. Guru, P. Joshi, S. Meena, J.R. Nadkarni, A. Singh, S.S. Bharate, S. Bhushan, S.B. Bharate, R.A. Vishwakarma, Pyrano- isochromanones as IL-6 inhibitors: synthesis, in vitro and in vivo antiarthritic activity, J. Med. Chem. 57 (2014) 7085–7097.
[17] M. Botta, S. Armaroli, D. Castagnolo, G. Fontana, P. Perad, E. Bombardelli, Synthesis and biological evaluation of new taxoids derived from 2- deacetoxytaxinine, J. Bioorg. Med. Chem. Lett. 17 (2007) 1579–1583.
[18] M. Rosner, K. Schipany, M. Hengstschläger, Merging high-quality biochemical fractionation with a refined flow cytometry approach to monitor nucleocytoplasmic protein expression throughout the unperturbed mammalian cell cycle, Nat. Protoc. 8 (2013) 602–626.
[19] A. Kamal, P. Suresh, A. Malla Reddy, B.A. Kumar, P.V. Reddy, P. Raju, J.R. Tamboli, T.B. Shaik, N. Jain, S.V. Kalivendi, Synthesis of a new 4-aza-2,3- didehydropodophyllotoxin analogues as potent cytotoxic and antimitotic agents, Bioorg. Med. Chem. 19 (2011) 2349–2355.
[20] M.A. Reddy, N. Jain, D. Yada, C. Kishore, J.R. Vangala, P. Surendra, A. Addlagatta, S.V. Kalivendi, B. Sreedhar, Design and synthesis of resveratrol based nitro vinyl stilbenes as antimitotic agents, J. Med. Chem. 54 (2011) 6751–6760.
[21] S.A. Innocente, J.L. Abrahamson, J.P. Cogswell, J.M. Lee, p53 regulates a G2 checkpoint through cyclin B1, Proc. Nat. Acad. Sci. USA 96 (1999) 2147–2152.
[22] A.P. Prakasham, A.K. Saxena, S. Luqman, D. Chanda, T. Kaur, A. Gupta, D.K. Yadav, C.S. Chanotiya, K. Shanker, F. Khan, A.S. Negi, Synthesis and anticancer activity of 2- benzylidene indanones through inhibiting tubulin polymerization, Bioorg. Med. Chem. 20 (2012) 3049–3057.
[23] A.R. Hamann, C. de Kock, P.J. Smith, W.A.L. Van Otterlo, M.A.L. Blackie, Synthesis of novel triazole-linked mefloquine derivatives: biological evaluation against *Plasmodium falciparum*, Bioorg. Med. Chem. 24 (2014) 5466–5469.
[24] N. Jain, Y. Divya, T.B. Shaik, G. Vasantha, P. Surendra Reddy, S.V. Kalivendi, B. Sreedhar, Synthesis and antitumor evaluation of nitrovinyl biphenyls: anticancer agents based on allocolchicines, Chem. Med. Chem. 6 (2011) 859–868.